Applied Surface Science 357 (2015) 819–831

Contents lists available at ScienceDirect

Applied Surface Science

journal homepage: www.elsevier.com/locate/apsusc

The antimicrobial efficiency of silver activated sorbents☆

Maja B. Đolić[a,*], Vladana N. Rajaković-Ognjanović[b], Svetlana B. Štrbac[c], Zlatko Lj. Rakočević[a], Đorđe N. Veljović[d], Suzana I. Dimitrijević[d], Ljubinka V. Rajaković[d]

[a] Vinča Institute of Nuclear Sciences, University of Belgrade, P.O. Box 522, 11001 Belgrade, Serbia
[b] Faculty of Civil Engineering, University of Belgrade, Bulevar Kralja Aleksandra 73, 11000 Belgrade, Serbia
[c] ICTM-Institute of Electrochemistry, University of Belgrade, Njegoševa 12, 11001 Belgrade, Serbia
[d] Faculty of Technology and Metallurgy, University of Belgrade, Karnegijeva 4, 11000 Belgrade, Serbia

ARTICLE INFO

Article history:
Received 7 July 2015
Received in revised form 3 August 2015
Accepted 2 September 2015
Available online 5 September 2015

Keywords:
Silver
Activated sorbents
Antimicrobial activity
E. coli
S. aureus
C. albicans

ABSTRACT

This study is focused on the surface modifications of the materials that are used for antimicrobial water treatment. Sorbents of different origin were activated by Ag^+-ions. The selection of the most appropriate materials and the most effective activation agents was done according to the results of the sorption and desorption kinetic studies. Sorption capacities of selected sorbents: granulated activated carbon (GAC), zeolite (Z), and titanium dioxide (T), activated by Ag^+-ions were following: 42.06, 13.51 and 17.53 mg/g, respectively. The antimicrobial activity of Ag/Z, Ag/GAC and Ag/T sorbents were tested against Gram-negative bacteria *E. coli*, Gram-positive bacteria *S. aureus* and yeast *C. albicans*. After 15 min of exposure period, the highest cell removal was obtained using Ag/Z against *S. aureus* and *E. coli*, 98.8 and 93.5%, respectively. Yeast cell inactivation was unsatisfactory for all three activated sorbents. The antimicrobial pathway of the activated sorbents has been examined by two separate tests – Ag^+-ions desorbed from the activated surface to the aqueous phase and microbial cell removal caused by the Ag^+-ions from the solid phase (activated surface sites). The results indicated that disinfection process significantly depended on the microbial-activated sites interactions on the modified surface. The chemical state of the activating agent had crucial impact to the inhibition rate. The characterization of the native and modified sorbents was performed by X-ray diffraction technique, X-ray photoelectron spectroscopy and scanning electron microscope. The concentration of adsorbed and released ions was determined by inductively coupled plasma optical emission spectroscopy and mass spectrometry. The antimicrobial efficiency of activated sorbents was related not only to the concentration of the activating agent, but moreover on the surface characteristics of the material, which affects the distribution and the accessibility of the activating agent.

1. Introduction

The pollution of water resources is the issue that demands the synergistic operation of engineers, chemists and biologists as it was accomplished within this research. So far, various natural materials are tested, in their native or modified forms, for removal of different water pollutants, such as: toxic metals [1,2], organic compounds [3], microorganisms [4] and simultaneous pollution removal applications [5,6]. Easily available and low cost sorbents are always attractive for heavy metals removal [7,8]. This is of great importance due to heavy metals non-biodegradability and tendency to accumulate in living organisms [9]. The absorption of organic species from aquatic medium was often conditioned by modification of the surface properties using different chemicals [10,11]. One of the most promising fields in water research is the potential application of sorbents activated by metal ions for antimicrobial activity, e.g. antimicrobial modified sorbents [12].

The water for human consumption is subjected to chemical and microbiological safety [13]. The World Health Organization (WHO), recommended that water intended for drinking should not contain fecal bacteria [14]. The presence of pathogenic microorganisms and infectious agents in the water is restricted, whether for drinking or recreation purpose [13,15]. For microbial destruction, or inactivation in the water different conventional methods of disinfections are applied. Lately, the special interest in this scientific field has been revived using metal-activated sorbents. The metal ions, such as: Ag^+, Cu^{2+}, Zn^{2+}, Sn^{2+}, Pb^{2+}, Ti^{2+} and Cd^{2+}, are

☆ *Disclaimer*: The content of this article is the authors' responsibility and neither COST nor any person acting on its behalf is responsible for the use, which might be made of the information contained in it.

* Corresponding author.
E-mail address: mirkovic.maja@gmail.com (M.B. Đolić).

http://dx.doi.org/10.1016/j.apsusc.2015.09.032
0169-4332/

well known as good antimicrobial agents and described as suitable antimicrobial carriers [16,17]. Inorganic materials have several advantages over traditionally used organic agents: chemical stability, thermal resistance, safety to the user, long lasting action period, etc. [18,19]. Among them, aluminosilicates and clays have been widely examined in antimicrobial activity, due to their high ion exchange capacity, high surface area and sorption capacity, negative surface charge, chemical inertness and low or null toxicity [18]. Zeolites, varied in origin and activated by Ag^{+}-, Cu^{2+}-, Zn^{2+}-, Ni^{2+}-, Sn^{2+}-, Pb^{2+}-, Bi^{2+}-, Cd^{2+}-, Cr^{3+}-, Fe^{3+}- and Ti^{4+}-ions, were one of the most used inorganic materials in different antimicrobial tests [4,12,17,20,21,22]. Montmorilonite, doped by silver, copper and zinc ions was suitable carrier for bacterial cell removal [23]. The clinoptilolite, previously Zn^{2+}-exhausted, was further applied in simultaneous phosphate removal and disinfection activity [15]. The untibacterial effect of sepiolite loaded by Cu^{2+}-nanoparticles was tested by Esteban-Cubillo et al. [24], showing 99.9% of *E. coli* and *S. aureus* cell removal. Activated carbons always have supreme position in final wastewater treatment step due to their large surface area. Ag^{+}-loaded activated carbon has showed very good antibacterial activity against *E. coli* and strong As (V) adsorption [16]. Li et al. performed modifications of Cu^{2+}, Zn^{2+} and Fe^{3+}-activated carbon and zeolite for enhanced *E. coli* removal from urban stromwater [12]. Ag^{+}-modified titanium-dioxide is one of the most widely used photocatalitic materials, applicable in various wastewater applications such as removal of organic water pollutants [25,26] and microbial and virus cell reduction in aquatic environment [27,28]. The metal-activated materials are not only used as disinfection carriers in the water treatment area, they are also proliferated in many segments of human activity. Zeolite, activated carbon and titanium dioxide, activated by Ag^{+}-, Cu^{2+}- and Zn^{2+}-ions are widely used for food preservation [29], while TiO_2 doped by silver ions found its utilization as self-desinfection fabrics [30].

This study is focused on Ag^{+}-activated sorbents that have potential application for the control of microbial growth in the aqueous system. In preliminary tests, 11 different materials: 5 natural-virgin (zeolite, sepiolite, bentonite, calcite and quartz), 3 natural-modified (powder activated carbon, granulated activated carbon and activated alumina) and 3 synthetic (artificial zeolite, titanium dioxide and ion exchange resin) were loaded by Ag^{+}-ions. Different antimicrobial aspects of pairs of sorbents and chemically active agents are critically observed. Also, the criteria for the selection of the most suitable carriers: natural (zeolite, Z), modified (granulated activated carbon, GAC) and artificial (titanium dioxide, T), by origin has been elucidated. Antimicrobial activity of Ag/GAC, Ag/Z and Ag/T sorbents were tested against Gram-negative bacteria *E. coli*, Gram-positive bacteria *S. aureus* and fungi *C. albicans*. In order to clarify the microbial cell reduction, the disinfection effect of Ag^{+}-ion was observed separately in aquatic medium (free Ag^{+} ions released from the sorbent) and on the activated surface (Ag^{+}-ions doped on the surface). Despite well known inhibition effect of free ions in aquatic solutions [9], in this study the disinfectant contribution of the activated surface to overall antimicrobial activity is emphasized.

The aim of this work was to evaluate silver activated sorbents that are the most suitable for bacteria and fungi cell removal and to demystify their antimicrobial activity. The main objectives of this work were: (i) the modification of the sorbent by simple metal loading process (Ag^{+}-activation process), (ii) the selection of the most suitable sorbents and chemical agents (toward adsorption and desorption kinetic studies), (iii) the investigation of structural changes of the activated materials and the chemical state of Ag^{+} activating agent, (iv) antimicrobial tests of the Ag^{+}-treated sorbents, (v) the clarification of the main cell reduction pathway and differentiation of the contribution of the Ag^{+}-ions released from the activated surface and Ag^{+}-ions loaded on the surface activated sites.

2. Materials and methods

2.1. The material selection and preparation

For the experiments in this study, 11 different materials were selected and divided in three main groups according to their origin:

(a) natural-virgin sorbents (labeled as group A, in Table 1): zeolite, Z (originating from Mare Baia, Romania, $(Na_{0.52}K_{2.44}Ca_{1.48})(Al_{6.59}Si_{29.41}O_{72})(H_2O)_{28.64}$), bentonite, B (originating from Birač, Zvornik, Bosnia and Herzegovina, $Na_{0.2}Ca_{0.1}Al_2Si_4O_{10}(OH)_2(H_2O)_{10}$), sepiolite, S (originating from Antići, Čačak, Serbia, $Si_{12}O_{30}Mg_8(OH)_4(H_2O)_4{\cdot}8(H_2O)$), calcite (originating from Central Bosnia and Herzegovina, $(Mg_{0.03}Ca_{0.97})(CO_3)$), and quartz sand, Q (River Sava basin, Belgrade, Serbia, alpha-SiO_2);
(b) natural-modified sorbents (labeled as group B in Table 1): powder activated carbon, PAC (Kemika, Zagreb, Croatia), granulated activated carbon, GAC (Karbozjak, Kruševac, Serbia), activated alumina, AL (Fisher Scientific, St. Louis, USA) and
(c) synthetic sorbents (labeled as group C in Table 1): artificial zeolite, AZ (Hopkin and Williams, London, Great Britain), titanium dioxide, T (Adsorbsia AS500, Dow, France) and ion exchange resin, IR (Amberlit Resin IR-120H, BDH England).

The main constituents and their content (expressed in %), BET specific surface area (expressed in m^2/g) and particle size (expressed in mm) distribution of the selected materials are presented in Table. 1 to provide deeper insight in adsorptive properties of tested materials.

Prior to their use, materials were washed by deionized water, dried for 2 h at 105 °C and placed in desiccators. The homogenization of dry sorbents was reached using mortar and pestle. Minimal number of processing steps for the material preparation was accomplished considering possible practical applications.

2.2. Characterization of the material

2.2.1. The X-ray diffraction

The X-ray diffraction (XRD) was used for the structural analysis of native and Ag^{+}-activated materials, employing an ENRAF NONIUS FR590 XRD (Bruker AXS, MA, USA) diffractometer with Cu K_α 1,2 radiation and a step/time scan mode of 0.05°/1 s. The XRD pattern of the native samples was compared with the diffraction powder file (PDF2) for activated carbon (reference pattern: 89-7213), clinoptilolite (89–7539) and titanium-dioxide (86-1157).

2.2.2. X-ray photoelectron spectroscopy

The X-ray photoelectron spectroscopy (XPS), used for the surface analysis of native and activated sorbents was carried out using SPECS System with XP50M X-ray source for Focus 500 and PHOIBOS 100/150 analyzer. AlKα source (1486.74 eV) at a 12.5 kV and 32 mA was used for this study. XPS spectra were obtained at a pressure in the range of 3×10^{-8} to 2×10^{-9} mbar. Survey spectra were recorded from 1000 to 5 eV, with the energy step of 0.5 eV, dwell time of 0.2 s, and with pass energy of 40 eV in the Fixed Analyzer Transmission (FAT) mode. Region spectra for each sample were taken from 360 to 380 eV, which include Ag 3d photoelectron lines. Region spectra were recorded with the energy step of 0.1 eV, dwell time 1 s and pass energy of 20 eV in the FAT mode. For Ag/Z and Ag/T samples, flow gun was used and adjusted to fit C 1 s energy of 284.8 eV. Spectra were collected by SpecsLab data analysis software and analyzed by CasaXPS software package both supplied by the manufacturer.

Table 1
The component profile (%), BET specific surface area (m^2/g) and particle size (mm) distribution of the selected materials.

Sorbent		Component, %	BET specific surface area, m^2/g	Particle size, mm	Ref
Natural materials					
	Zeolite (Z)	Clinoptilolite, 80	45.7	0.4–0.8	[31]
	Bentonite (B)	SiO_2, 55 Al_2O_3, 16.8	59.3	<0.074	[32]
A. Virign	Sepiolite (S)	SiO_2, 57 MgO, 28.6	268	<0.074	[32]
	Calcite (C)	$CaCO_3$, 85	9.8	0.001	Present study
	Quartz (Q)	SiO_2, 76	2.6	0.20–0.55	Present study
	Powder activated carbon (PAC)	Carbon, 91.9	1014	0.023	[33]
B. Modified	Granulated activated carbon (GAC)	Carbon, 63.3	1436	0.355–1.60	[34]
	Activated alumina (AL)	Al_2O_3, 90	230	0.50–2.00	Present study
Synthetic materials	Artificial zeolite (AZ)	/	280	0.45–1.50	Present study
	Titanium-dioxide (T)	Titanium-dioxide, 89	250	0.25–1.25	[35]
	Ion exchange resin (IR)	/	300	0.354–0.841	Present study

2.2.3. Scanning electron microscopy

After the deposition of a thin gold layer on the native and activated sorbents, a TESCAN MIRA 3 XMU field emission scanning electron microscope (FE-SEM), operated at 20 keV, was used to analyze the morphology of the samples.

2.3. Activation process

2.3.1. Reagents

Chemical of analytical grade Ag_2SO_4 was supplied by Merck (Darmstadt, Germany), and HNO_3 from Sigma Aldrich (St. Louis, MO, USA). Ultra-pure water produced by a Millipore Milli-Q system (the resistivity 18 MΩ cm^{-1}), was used throughout the experimental work in sorption and desorption processes.

2.3.2. Sorption experiment

Set of adsorption experiments, in the singular batch mode, was tested in order to compare sorption capacity of 11 different sorbents for Ag^+-ions. Standard solution of Ag_2SO_4 was prepared by dissolving 1 g of sulfate salt in 1 L of deionized water; concentration of 3.2 mmol/dm^3 was obtained. Experiments were performed following the standard procedure: 1.00–4.00 g of solid sample was added to 100 mL of standard solution of metal. The sorption process was stimulated by orbital shaker by stirring at 170 rev min^{-1} (Heidolph ROTAMAX 120), at room temperature 21 ± 1 °C, over a period from 3 min to 24 h. Adsorption studies were conducted under acidic conditions (pH = 5.5). Concerning silver ions, acidic conditions preserve Ag^+-ions to form black precipitate Ag_2O, which is formed as a result of the reaction of silver cation and the hydroxide anion yielding AgOH, according to the reactions (1) and (2):

$$Ag^+ + OH \rightarrow AgOH \quad (1)$$

$$2AgOH \rightarrow H_2O + Ag_2O(\text{blackprecipitate}) \quad (2)$$

Intermediate acidic conditions enable Ag^+-ions to be removed from the solution by adsorption process, avoiding the effect of precipitation [36]. The aliquots of 1 mL were taken at 3; 5; 10; 15 and 30 min from the beginning of the process; as well as after 1; 2; 3; 4; 5; 6; 8; 12 and 24 h. After final activation period (24 h), sorbents and solutions were separated by filtration through the standard filter designed for a wide range of laboratory applications (MF-Millipore membrane filter, mixed cellulose ester, 0.45 μm). Sorbents were exposed to ambient conditions for 24 h and dried on 105 °C for 2 h. All, 33, activated samples were weighted to four digit accuracy (Radwag model mza5.3y, Radom, Poland) before the next step – desorption experiment. The filtrates and the aliquots were collected and the concentrations were measured by inductivity coupled plasma optical emission spectroscopy (ICP-OES).

2.4. Desorption experiment

The kinetic behavior of the released Ag^+-ions was studied in a similar manner, in the singular batch mode. Each sorbent, previously dried and measured, after sorption process, was submerged with 100 mL of distilled water at 20 ± 1 °C over a period from 3 min to 24 h. The aliquots of 1 mL were taken at 3; 5; 10; 15 and 30 min from starting time; as well as after 1; 2; 3; 4; 5; 6; 8; 12 and 24 h. The samples were gently stirred at 50 rev min^{-1} by orbital shaker. After final desorption period of 24 h, the sorbents and solutions were separated, filtrated and dried, following the same procedure as the activation step. The aliquots, 14 measurement points, were collected using microtubes of 1.5 mL volume. Phase removal (solid particles in aliquots) was performed using ultracentrifuge (Heraeus Sepatech Biofuge 13) on 12,000 rpm for 5 min and the concentrations of metal ions in supernatant were analyzed by induced coupled-mass spectrometry (ICP-MS).

2.5. The metal ions concentration determination

2.5.1. The concentration of residual metal ions after sorption process

The aqueous phase concentrations of Ag^+-ions were detected by inductively coupled plasma optical emission spectroscopy (ICP-OES) on *Thermo iCAP 6500 system*, equipped with the Thermo iTEVA software, a concentric nebulizer, and a Cyclonic Spray Chamber. External calibration with standards prepared from Certipur Merck 1000 mg/L, single standard solutions, was applied for the measurements. Calibration blank, calibration standards and samples were acidified with 65% nitric acid (Trace Select from Sigma-Aldrich) to final adjustment to 2% nitric acid. The detection limit for Ag^+-ions was 0.02 mg/L, operating on 328.068 nm. Samples for Ag measurements were collected in amber vials. These solutions were acidified, centrifuged and the concentrations of Ag^+-ions were measured after the experiments were accomplished. The accuracy and precision of the measurement were controlled using LGC ERM-CA011 reference material.

2.5.2. The concentration of released metal ions after desorption process

The concentration of Ag^+-ions was determined using Thermo iCAP Qc ICP-MS. External calibration was used with calibration standards prepared from 1000 mg/L single element Merck solutions for each analyzed ion. Calibration standards were prepared with 1% HNO_3 as a diluent (Fluka Analytical Trace Select HNO_3). As internal standard Indium was used. After every tenth measurement continuing calibration verification solution (CCV) was analyzed in order to verify the integrity of the instrument calibration. CCV was prepared from the Accu standard ICP multi element standard MES

21-1. Certified reference material ERM CA011b was measured undiluted to verify the overall performance of the measurements and these values were within 85–115% which is acceptable according to EPA 200.8.

2.6. Efficiency of sorption and desorption processes

2.6.1. The sorption capacity

Sorption capacity (SC) of activated materials for Ag^+-ions, expressed in mg of doped metal per g of sorbent, is calculated from Eq. (1):

$$SC = \frac{(C_O - C_S)}{m} V \quad (1)$$

where *Co* (mg/L) is an initial element concentration (in the standard solution), and *Cs* (mg/L) is concentration after 24 h of activation process. The *V* (L) is volume of contact solution (standard solutions) and *m* (g) is the mass of examined sorbent. The SC is a specific characteristic for each type of sorbent and depends on the nature of material and of chemical agent.

2.6.2. The desorption capacity

The desorption capacity (DC) for analyzed materials, expressed in mg of released metal per g of sorbent is calculated from Eq. (2):

$$DC = \frac{C_d}{m'} V \quad (2)$$

where C_d (mg/L) is the total desorbed concentration after 24 h, *V* (L) is the volume of contacting solution and m' (g) is the mass of activated material, after sorption process.

2.7. Microbiological tests

2.7.1. Reagents and microbial culture

Antimicrobial activity was tested against microbiological cultures: Gram-negative bacteria, *E. coli* (ATCC 25922, Microbiologics, USA), Gram-positive bacteria, *S. aureus* (ATCC 25923, Microbiologics, USA) and fungi *C. albicans* (ATCC 24433, Microbiologics, USA). Solid substrates for *E. coli* and *S. aureus* were prepared by Plate count agar (Torlak, Serbia)., while Sabouraud malotose agar was used for C. albicans growth (Torlak, Serbia). Analytical grade, sodium chloride, NaCl, was supplied by Merck (Darmstadt, Germany).

2.7.2. Antimicrobial tests for Ag^+-activated sorbents

The antimicrobial activity of Ag^+-activated sorbents was evaluated against *E. coli*, *S. aureus* and *C. albicans* using the standard test dilution. Briefly, a mass of 0.1 g of each activated sorbent (Ag/GAC, Ag/Z and Ag/T) was added to a tube containing 9.9 mL of sterile 0.9% NaCl solution (pH 6.2). The saline was inoculated with 0.1 mL of an overnight culture inoculum. The tubes were incubated in a water bath shaker (Memmert, Germany) at 150 rpm, for 15–20 min, at 37 °C. The aliquot of 0.1 mL of the mixture, saline, activated sorbent and inoculum, was diluted in the 9.9 mL of the saline. Other, different dilutions were also performed. From each dilution, the 0.1 mL aliquot was placed in a Petri dish and covered with appropriate agar. After 15 min of the incubation at 37 °C, the number of surviving microorganism colonies was counted. As a control sample, a blank sterile saline with a native sorbent was used.

2.7.3. Antimicrobial tests for aqueous phase with released Ag^+-ions

Inactivation of *E. coli*, *S. aureus* and *C. albicans* by released Ag^+-ion in aqueous phase was also investigated. Antimicrobial tests were performed by different concentrations of free Ag^+-ions, collected after 15 min of desorption period of Ag/GAC, Ag/Z and Ag/T. Test tubes were inoculated with 0.1 mL overnight culture inoculums. After incubation period at 37 °C, the aliquot of 0.1 mL was diluted in the 9.9 mL of the saline. The dilution test is performed as described in the previous paragraph. A control sample, without Ag^+-ion was performed under the same conditions, in saline.

2.7.4. Estimation of antimicrobial activity

The degree of the microbial cell reduction (*R*, %) was calculated according to Eq. (3):

$$R(\%) = \frac{[CFU_{cont} - CFU_m]}{CFU_{cont}} 100 \quad (3)$$

where CFU_{cont} is the number of microorganism colonies in the control sample with native sorbents or only with saline, and CFU_m is the number of microorganism colonies in the tubes with silver activated samples (Ag/GAC, Ag/Z, Ag/T) or with Ag^+-ions released from the activated surface.

All antimicrobial tests were performed in triplicate. The mean value and standard deviation were calculated by Origin Pro software (OriginLab Corporation).

Table 2
Activation (sorption) and desorption capacities of 11 different sorbents for Ag^+-ions, after 24 h of duration time.

Sorbent		Activating ion	
		Ag^+	
		SC, mg/g	DC, mg/g
Natural materials			
	Zeolite (Z)	13.51	0.085
	Bentonite (B)	3.28	0.30
A. Virign	Sepiolite (S)	15.29	0.03
	Calcite (C)	7.15	0.04
	Quartz (Q)	4.23	0.68
	Powder activated carbon (PAC)	16.16	0.04
B. Modified	Granulated activated carbon (GAC)	42.06	0.32
	Activated alumina (AL)	6.52	0.011
	Artificial zeolite (AZ)	15.83	0.009
Synthetic materials	Titanium dioxide (T)	17.53	1.05
	Ion exchange resin (IR)	21.18	0.043

Metal ion	SC (mg/g)	DC (mg/g)
Ag^+	**GAC**>IR>**T**>PAC>AZ>S>**Z**>C>AL>Q>B	**T**>Q>**GAC**>B>**Z**>IR>C∼PAC>S>AL∼AZ

Table 3
Sorption capacity of activating components in different modified sorbents and their minimum inhibitory concentrations in antimicrobial activity.

Material	Activating component	Sorption capacity (mg/g)	MIC (mg/mL)	Exposure period, h	Antimicrobial activity	Ref.
Zeolite X	Ag^+	20.0	0.15; 0.15; 0.15	1; 1; 1	*E. coli*; *P. aeruginosa*; *S. eureus*	[22]
Zeolite X	Ag^+	98.0	0.3; 0.3; 1.0; 1.0	24; 24; 48; 48	*E. coli*; *B. subtilis*; *S. cerevisiae*; *C. albicans*	[41]
Zeolite Y	Ag^+	97.0	0.2; 0.2; 1.0; 1.0	24; 24; 48; 48	*E. coli*; *B. subtilis*; *S. cerevisiae*; *C. albicans*	[41]
Clinoptilolite	Cu^{2+}	26.0	10.0; 10.0	24; 24	*E. coli*; *S. eureus*	[4]
Clinoptilolite	Ni^{2+}	5.20	10.0; 10.0	24; 24	*E. coli*; *S. eureus*	[4]
Clinoptilolite	Zn^{2+}	13.0	10.0	24	*A. junii*	[5]
Sepiolite	Cu^{2+}	10.0	/	24	*E. coli*; *S. aureus*	[24]
Montmorilonite	Ag^+	33.6	2.5	24	*E. coli*	[18]
Montmorilonite	Zn^{2+}	/	0.5; 0.5	24; 24	*Pycnoporus cinnabarinus*; *Pleurotus ostreatus*	[23]
GAC	Ag^+	10.0	0.016	24	*E. coli*	[6]
GAC	Ag^+	24.7	0.5	0.17	*E. coli*	[44]
GAC	Ag^+	16.5	0.02	24	*E. coli*	[45]
TiO_2/citozan	Ag^+	50.0	0.00038	24	*E. coli*	[29]
TiO_2	Ag^0	/	10.0; 10.0; 10.0	24; 24; 24	*E. coli*, *S. aureus*, *C. albicans*	[30]
TiO_2	Ag^+	10.0	0.001	24	*E .coli*	[46]

3. Results and discussion

3.1. Preliminary investigations

Sorption and desorption capacities of 11 sorbents loaded by Ag^+-ions, after 24 h are presented in Table 2. The efficacy of activation process is determined by sorption capacities (SCs). Virgin natural sorbents were analyzed in preliminary investigation in greater scope due to availability and possible easier implementation. But, the analysis showed that natural-modified and synthetic materials have higher affinity for metal ions, than the virgin ones. The range of SCs was: 42.06–3.28 mg/g for Ag^+-ions. The high affinity was manifested for Ag^+-ions, which is related to hydrated ionic diameter phenomenon [21]. Hydrated radius is inversely proportional to cationic radius. The value of silver cationic radius is 1.13 Å which indicates that hydrated radius of Ag^+-ion has an advantage for easier absorption by sorbent [37]. The affinity of each tested material for silver ion was also considered and is presented in the lower part of Table 2. Desorption studies give information on the concentration of released ions into the solution. The slow release of metal ions from the activated surface is followed by an antimicrobial effect. Supporting this phenomenon, the presence of free ions after desorption was analyzed in distilled water. The range of DCs was: 1.05–0.009 mg/g for Ag^+-ions. These results indicate that DSc are nearly 20 (for titanium-dioxide) to 2000 (for artificial zeolite) times lower then SCs of the same materials. Low desorption rate of heavy metals, adsorbed or naturally present in minerals, was proved in our previous study [38]. Desorption of metal ions by the natural virgin and modified material did not show any specific order.

Regarding SCs and DCs obtained for Ag^+-ions, as well as the differences in the origin of examined materials, for further antimicrobial tests *Z* (particle size 0.4–0.8 mm), as a representative of natural virgin sorbent, GAC (particle size 2–4 mm), a natural modified sorbent and T (particle size 0.25–1.2 mm), as a synthetic sorbent, were selected. One of the criteria for the selection of appropriate sorbent, beside proven antimicrobial efficacy, is sorbent stability and its lifetime [12]. In this study, sorbents of different desorption rates are intentionally selected because the release of Ag^+-ions will determine the pathway of overall antimicrobial activities.

3.2. Critical overview of the previous silver antimicrobial studies–alleviation of the differences

The selection of appropriate sorbents and activating agent depends on several parameters: SC (quantity of the surface loaded activating agent) [16,21]; desorption kinetics (stability of the sorbent – slow release of free metal ions) [17,22,39]; chemical state of the activating agent (Ag^0 vs. Ag^+) [18,40,41] and structural properties of the material (better porosity enables better distribution of the Ag^+-ions through the material and easier accessibility of the activating agent to the microbial solution) [4,18,40]. Taking into account all of the above, the appropriate sorbent selection and their microbiological testing depends on many factors. The selection of different materials, activating components, sorption capacities of the modified sorbents and minimum inhibitory concentration (MIC), used in some previous antimicrobial investigations are presented in Table 3.

Successful activation process, e.g. good sorption capacity for specific metal is a prerequisite for the choice of adequate activating agent (metal ion selection). Metal ions (Ag^+, Cu^{2+}, and Zn^{2+}) provide efficient microbial cell reduction [22,23]. In literature, there are opposite explanations related to the explanation of antimicrobial activity. At first, microbial cell reduction was explained by conventional approach that free metal ions inactivate bacteria and fungi cell growth [9,22,42]. But, lately, the contribution of the activated material on antimicrobial activity has also been evaluated [4,12]. Within this study both influences are considered, cell reduction due to free ions in solution [22,23] and the antimicrobial effect of the ions doped on the surface of sorbent [18,41]. These two steps do not exclude each other, e.g. they are complementary. Although some of previous investigations indicated similar conclusion [4], this phenomenon has not been yet clarified. The kinetic study of released ions from the surface enables the clarification of antimicrobial mechanism of activated sorbents.

In some of the previous studies the importance of the chemical state of the activating agent for the antimicrobial activity was appointed [40,41,43]. Inoue et al. investigated antibacterial activity of silver activated zeolite and discovered that the bactericidal activity was very low when oxidation state of silver was zero [43]. Ferreira et al. discovered that the ratio of present silver ions and elemental silver (e.g. Ag^+/Ag^0 atomic ratio) on the activated surface determined an overall antimicrobial effect. Nevertheless, the porosity of materials and distribution of the chemical agent dictated the accessibility of the activating agent [4,40]. Magana et al. focused on the influence of the porosity on antimicrobial effect of the montmorilonite (calcined and milled) [18]. Better inhibition rate was obtained by calcined clay where Ag^+/Ag^0 atomic ration was lower. This could be directly the consequence of Ag^+-ion incorporation in the interlayer of the calcined sample and non-homogeneous profile distribution of the activating agent. Beside metal ion activating treatment, impregnation of materials by film of oxides or hydroxides [12] is often used procedure for sorbent modification.

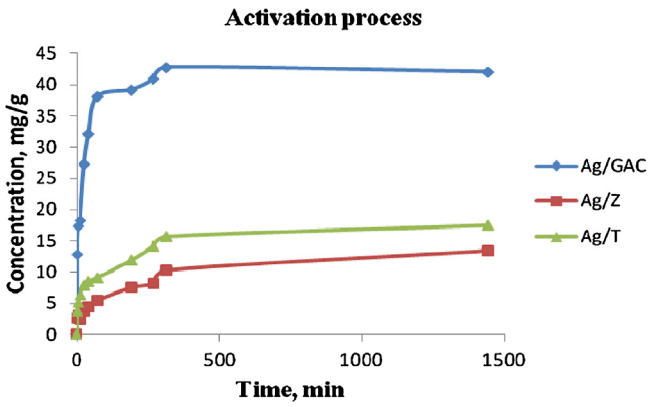

Fig. 1. Activation process of GAC, Z and T sorbents by Ag^+-ions.

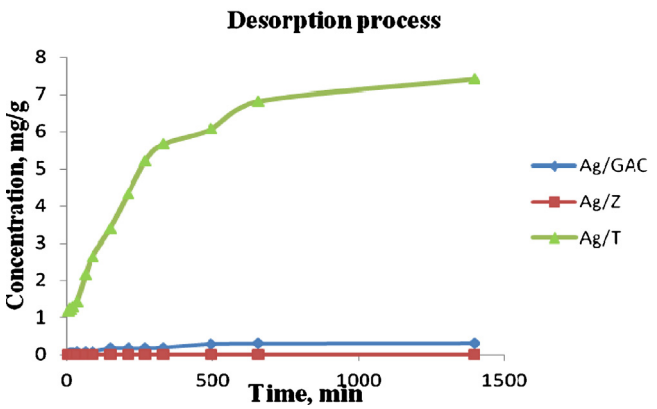

Fig. 2. Desorption process of Ag^+-ions, released by Ag/GAC, Ag/Z and Ag/T sorbents.

The metal hydr(oxide) coating approach provides better sorbent stability in water due to its low solubility constant [37]. The slower release of metal ions from the hydr(oxide) activated surface into the solution may affect microbial removal for a longer time. Sorption capacity of hydr(oxide) layered sorbents proved to be lower than metal-activated materials [12].

3.2.1. Material activation by Ag^+-ions and sorption process efficiency

The activation process, with Ag^+-ions as chemical agent and GAC, Z and T as selected sorbents, was performed in singular batch mode. The change of sorption capacity of Ag/GAC, Ag/Z and Ag/Z, with time, during 24 h, for activation process, is shown in Fig. 1.

Comparing the sorption capacities of GAC, Z and T sorbents for Ag^+-ions, the values were: 42.06, 13.51 and 17.53 mg/g, respectively. The applied activation process was very efficient for Ag/GAC and satisfactory for Ag/T and Ag/Z. After 24 h, 65% of Ag^+-ions were loaded on GAC, while 27 and 21% were adsorbed onto T and Z sorbents. The change of the sorption capacity per time can be fitted by kinetic models of pseudo-first and pseudo-second order. Both kinetic models gave a similar sorption trend. Using GAC sorbent, 50% of initial Ag^+-ions were removed from the solution after 45 min, while Z and T showed slower sorption kinetics, 50% of Ag^+-ions were uptaken in 3 h and 2 h, respectively. From the obtained values of sorption efficiency and kinetic parameters for the activation process, Ag^+-ions are the most suitable choice for chemical activating agent.

3.2.2. Desorption of the Ag^+ ions from the activated surface

Desorption kinetic studies give the information based on the change of concentration of released Ag^+-ions per time. Slow release of metal ions enables stability and longevity of the activated sorbent. The release of free Ag^+-ions was simulated in deionized water, at pH 5.5 during 24 h. Desorption kinetic studies of Ag/GAC, Ag/Z and Ag/T are shown in Fig. 2.

Comparing desorption capacities of Ag/GAC, Ag/Z and Ag/T, expressed in mg/g the values obtained were: 0.32, 0.008 and 7.41, respectively. There is obvious difference in Ag^+-ions release tendency between selected materials. Ag/Z exhibits low desorption rate, while Ag/GAC has moderate desorption rate of Ag^+-ions in contrary to Ag/T, with high desorption rate. For this study, these differences in the desorption rates of selected materials are convenient for the analysis and explanation of the contribution of the activated sorbent (activated sites on the surface of the material) to antimicrobial activity. Separate analysis of the microbial cell removal caused by the Ag^+-ions from the aqueous phase and Ag^+-ions from the solid phase will be performed. The important distinction in this approach is related to the chemical state of the activating agent. Structural and surface analysis of native and Ag^+-activated sorbents provides better insight in the mechanism of antimicrobial activity.

3.3. Structural and surface properties of activated sorbents

3.3.1. XRD analysis

The results of XRD analysis of native, GAC, and activated, Ag/GAC sorbent are shown in Fig. 3. The analysis showed that silver activated sorbent has been subjected to structural change. The presence of elemental silver (Ag^0) has been detected at characteristic peaks: $2\theta = 38.10^\circ$; 44.25° and 64.40° [44,45]. The broad peaks of GAC and the sharp peaks of silver appeared in the pattern of the Ag/GAC refer to the coexistence of the both Ag/GAC and GAC [6]. Silver ions (Ag^+) from the activation medium, Ag_2SO_4 solution, were adsorbed on GAC surface and they have been reduced by carbon atoms, a strong reducing agents, to elemental silver (Ag^0) [47]. This reaction explains the chemical state of the activating agent which is loaded as metallic silver on Ag/GAC activated surface. The appearance of two new peaks, at $2\theta = 20.95^\circ$ ($(Na,K)_2S_2O_3$) and $2\theta = 23.30^\circ$ (S), are also a consequence of reduction process of the sulfate group (SO_4^{2-}) from the activation medium.

The results of XRD analysis of native, Z, and activated, Ag/Z sorbent are shown in Fig. 4. The analysis has shown that there were no significant structural changes between natural and activated sorbent, except for the silver peak which appeared when activated sorbent has been analyzed. The diffraction pattern of modified sorbent has peaks ($2\theta = 10.00^\circ$ and 22.55°) which are less intensive then the peaks for the natural sorbent. This is the consequence of the presence of different silver states, elemental silver (Ag^0) and

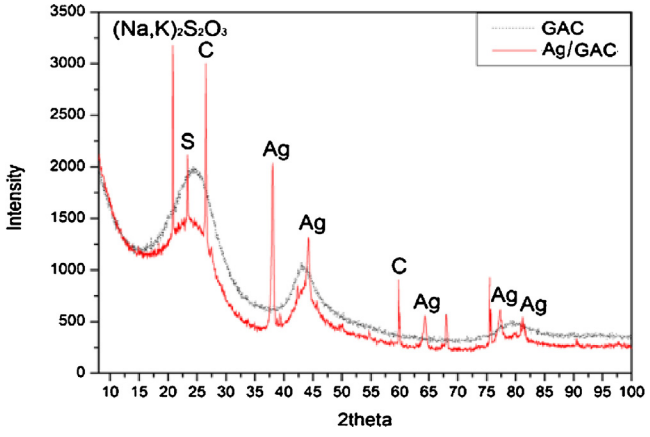

Fig. 3. XRD analysis of GAC (dashed line) and Ag/GAC sorbent (solid line).

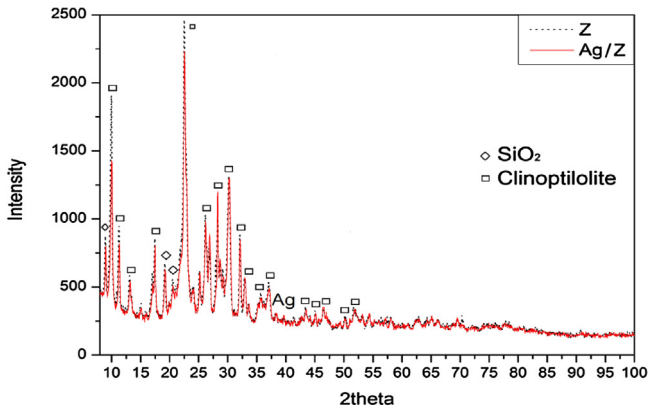

Fig. 4. XRD analysis of Z (dashed line) and Ag/Z sorbent (solid line).

ionic silver (Ag^+) [41]. Moreover, low intensity of elemental silver, characteristic peak at $2\theta = 38.10^\circ$, indicated lower amount of silver in the zeolite framework and higher dispersion of the metal inside zeolite hosts [41]. Silver in ionic state was not noticed by XRD analysis, but complementary XPS technique has confirmed its presence.

The results of XRD analysis of native, T, and activated, Ag/T sorbent are shown in Fig. 5. The analysis showed that there were no significant structural changes between synthetic and activated sorbent. The characteristic peak of titanium-dioxide has been observed at $2\theta = 25.30^\circ$. The diffraction pattern of Ag/T indicated that silver is present in activated sorbent as ionic silver, in form of silver (I, III) oxide, AgO, detected at $2\theta = 32.50^\circ$ [48]. Although its empirical formula, AgO, suggests that silver is in the +2 oxidation state in this compound, silver (I, III) oxide is a mixture of two silver oxides and is formulated as $Ag^{I}Ag^{III}O_2$ or $Ag_2O{\cdot}Ag_2O_3$ [49]. The confirmation of the presence of silver in ionic state in Ag/T sorbent has also been the subject of XPS analysis.

3.3.2. XPS analysis

XPS spectra of activated, Ag/GAC sorbent are presented in Fig. 6. In Fig. 6a the survey spectrum shows the positions of oxygen, carbon and silver elements. The analyzed sample consists mainly of carbon with the atomic percentage (inseted table) of 93.3%. Although the sample has 4.5 At % of oxygen, and 2.2 At % of silver, according to the position of Ag $3d_{5/2}$ photoelectron line at 368.14 eV, and Ag $3d_{3/2}$ at 374.17 eV, Fig. 6b, silver is in its metallic state [44,50].

XPS spectra of activated, Ag/Z sorbent are presented in Fig. 7. In Fig. 7a the survey spectrum shows photoelectron lines of the main elements and their atomic percentage in the insert. The

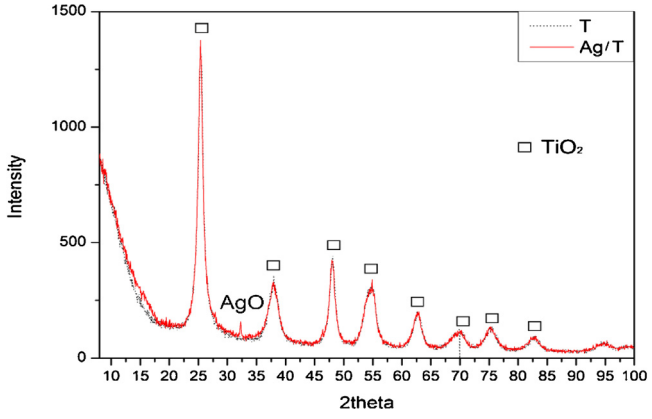

Fig. 5. XRD analysis of T (dashed line) and Ag/T (solid line).

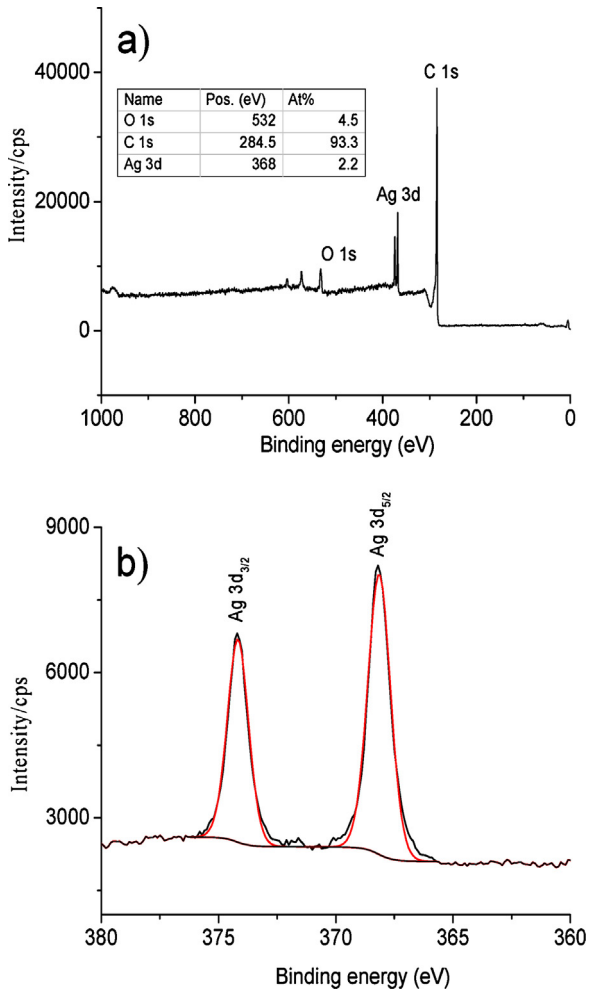

Fig. 6. XPS spectra of Ag/GAC sample: (a) the survey spectrum with the position and the atomic percentage of the main components; (b) high resolution region spectrum of Ag 3d showing the fitted binding energies.

atomic percentage of silver is 0.7%, and the region spectrum (in Fig. 7b) shows Ag 3d lines. These, Ag 3d, lines are fitted into two contributions, indicating the simultaneous presence of both chemical states of silver. The position of Ag $3d_{5/2}$ lines at 371.1 and 368.0 eV, can be attributed to the metallic silver (Ag^0) and silver (I, III) oxide, in form of AgO, respectively [51,52]. Metallic silver was also detected by XRD analysis, while the presence of Ag^+ signal could be attributed to the silver ions interchanged in the hosts of structure of Ag/Z. Similarly, Ag $3d_{3/2}$ lines are fitted into two contributions positioned at 376.9 and 374.3 eV corresponding to metallic silver (Ag^0) and AgO, respectively [52].

XPS spectra of activated, Ag/T sorbent are presented in Fig. 8. In Fig. 8a the survey spectrum shows the positions of oxygen, titanium, silver and carbon. The atomic percentage of each component is given in the insert. The position of the Ti 2p peak at 457.5 eV, close to Ti $2p_{3/2}$ at 458.0 eV corresponds to a +4 oxidation state in titanium dioxide, TiO_2 [26,53] which is in accordance with a bit more than two times higher atomic percentage of oxygen. The oxygen also resulted in oxidation of silver which is present in the form of oxide AgO. High resolution XPS spectrum of Ag 3d region is presented in Fig. 8b. Fitted Ag $3d_{5/2}$ photoelectron line positioned at 367.3 eV, with symmetrical shape before and after activation process, corresponds to the silver ionic state of AgO [25]. The results obtained from XPS analysis correspond to XRD structural analysis.

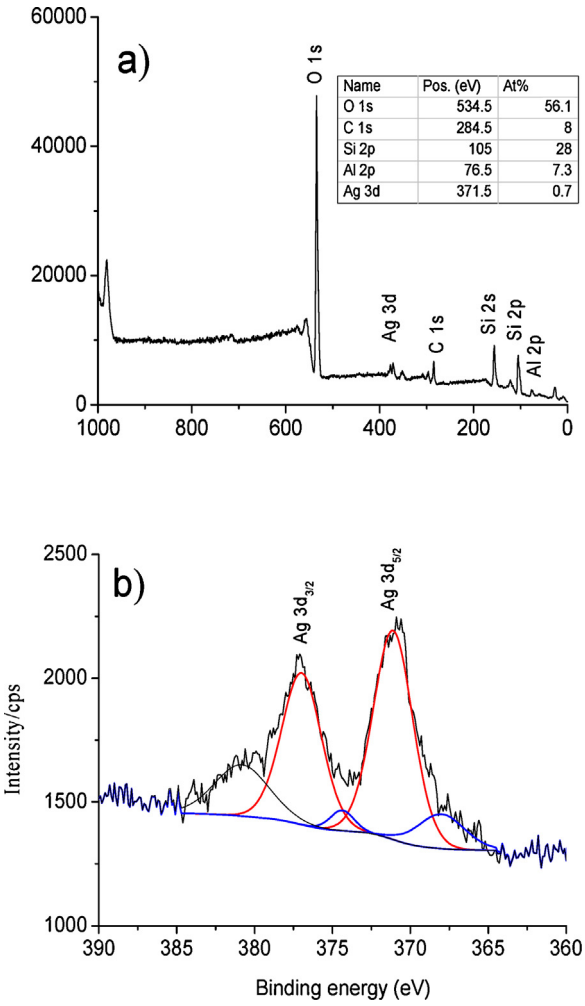

Fig. 7. XPS spectra of Ag/Z sample: (a) the survey spectrum with the position and the atomic percentage of the main components; (b) high resolution region spectrum of Ag 3d showing the fitted binding energies.

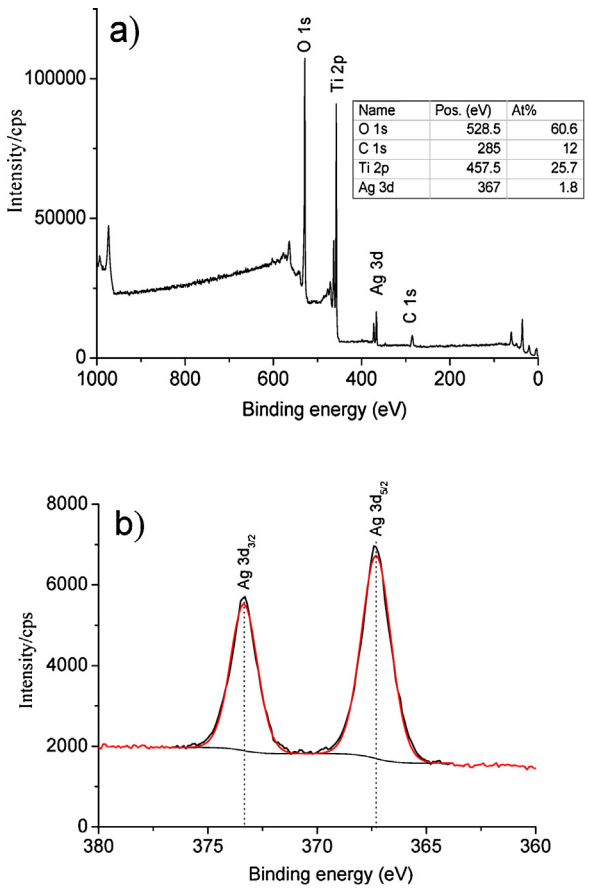

Fig. 8. XPS spectra of Ag/T sample: (a) the survey spectrum with the position and the atomic percentage of the main components; (b) high resolution region spectrum of Ag 3d showing the fitted binding energies.

3.3.3. SEM analysis

The surface morphology of the native, GAC and activated sorbents, Ag/GAC was investigated by FE-SEM technique. Representative FE-SEM images of GAC and Ag/GAC are shown in Fig. 9. GAC sample consists of many particles with random forms and sizes [6]. After Ag^+-activation process, FE-SEM images showed the presence of white nanoparticles on the surface of Ag/GAC, with the particle size of diameter less than 200 nm. The distribution of the particles is pretty homogeneous. The characteristic layout of the silver particles on Ag/GAC, aggregated in regular shapes of squares, triangles and circles, indicate that elemental silver has formed crystallites on the sorbent surface [18]. This analysis is in agreement with XRD and XPS techniques, which confirmed the presence of metallic silver (Ag^0) on the Ag/GAC surface.

Representative FE-SEM images of the native, Z and silver activated zeolite, Ag/Z are presented in Fig. 10. The surface morphology of zeolite confirmed the presence of different particle shapes and sizes, which commonly appear in complex inorganic crystalline structures such as natural clinoptilolites [16]. The differences in micrographs of native, Z, and activated sorbent, Ag/Z, are result

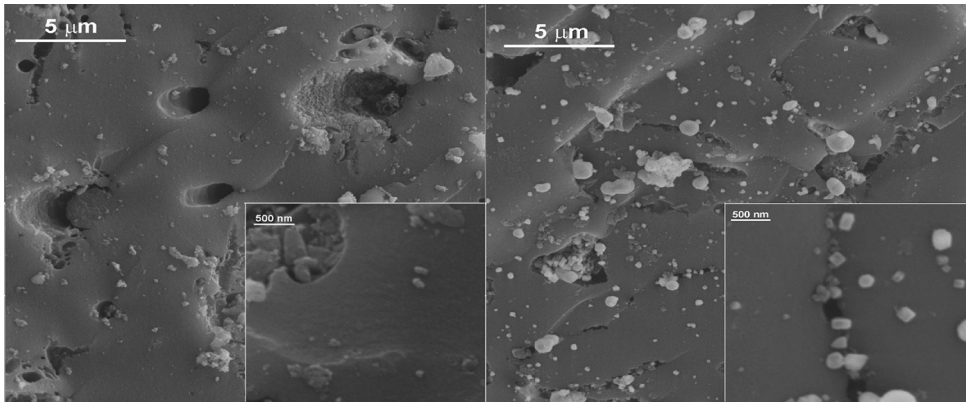

Fig. 9. FE-SEM image of GAC (on the left) and Ag/GAC (on the right) with 10,000 and 70,000 times enlargement (incorporated picture).

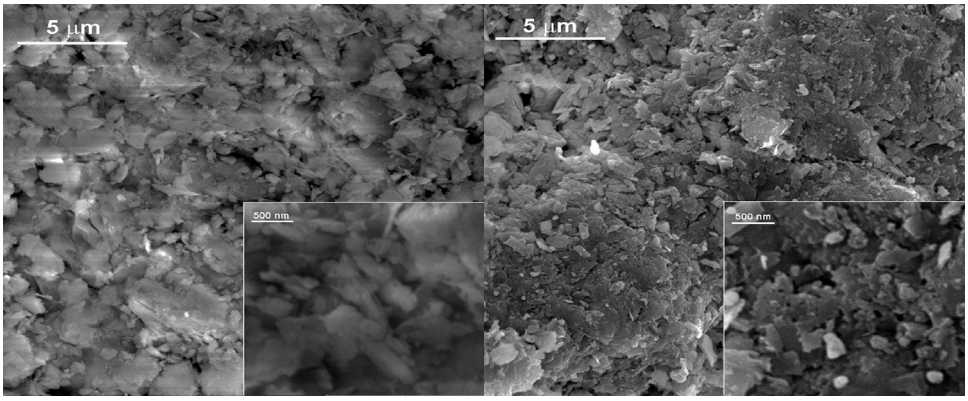

Fig. 10. FE-SEM image of Z (on the left) and Ag/Z (on the right) with 10,000 and 70,000 times enlargement (incorporated picture).

of Ag^+-activating agent, previously confirmed by XRD and XPS analysis. The presence of metallic silver has been detected through white particles, irregularly spread on the surface of the Ag/Z sorbent. Similar results of the silver activated zeolite surfaces have been already reported [18].

Representative FE-SEM analysis of native, T and activated, Ag/T sorbents are presented in Fig. 11. The surface morphology of the native and activated titanium-dioxide consists of similar, regular shaped particles [29]. After activation process, the micrographs of the Ag/T surface exhibited slight increase in the number of white spots, which indicates the presence of the silver. Although FE-SEM images did not clearly show the presence of the silver on Ag/T surface, XRD and XPS analysis confirmed the presence of the ionic silver on the activated sorbent. Moreover, XPS analysis provided the information about the atomic percent of the silver loaded on Ag/T, 1.8% (Fig. 8, inserted table).

3.4. Antimicrobial tests

The antimicrobial activity of the sorbents activated by Ag^+-ions, has been observed through the reaction of metal ions loaded on the surface of the sorbent and free metal ions detached from the activated surface in aqueous phase. Slow and continuous release of silver ions in the microbial environment is critical factor needed to ensure the antimicrobial efficacy [22,42]. Simultaneously, metal activated sorbents tend to attract the negatively charged membranes of the bacteria to the surface of the material, where the positive charged silver ions inactivate microbial or enable them to replicate [4,12,17]. With this study, an attempt to make a distinction between the contribution of the Ag^+-ions from the aqueous phase and Ag^+-ions from the activated surface to antimicrobial activity. In order to achieve this, two separate experiments were performed: antimicrobial tests of the activated sorbents (Ag^+-ions from the solid phase) and antimicrobial tests of Ag^+-ions from the aqueous phase. For the low release rate of Ag^+-ions, it could be expected that an antimicrobial effect is a consequence of the presence of Ag^+-ions on the surface (activated sites are responsible for the microbial cell reduction). For sorbents with high desorption rate of Ag^+-ions, the cell inactivation is related to the presence of desorbed Ag^+-ions into the microbial solution.

3.4.1. Antimicrobial activity of Ag^+-activated sorbents

The antimicrobial activity of Ag-activated materials was tested in three different stages of their exhaustion. Ag/GAC, Ag/Z and Ag/T sorbents were tested with maximum Ag^+-load: after 24 h of sorption process (labeled as sample 24S, in Table 4), after 6 h of desorption period (sample labeled as 06D, in Table 4) and after 24 h of desorption period (sample labeled as 24D, in Table 4). In order to ensure that the reduction of both bacteria and yeast is exclusively the consequence of antibacterial activity of activated sorbents, experiment was performed in dark. The exposure period was limited to 15 min, to minimize desorption of free Ag^+-ions in the solution, e.g. to minimize the effect of released Ag^+-ions to antimicrobial activity.

Cell reduction was the most successful using Ag/Z sorbent. For *E. Coli* the reduction reached 90.7, 92.2 and 93.5%, for the samples 24S, 06D and 24D, respectively (Table 4). The inhibition rate for *S. aureus*, in three different steps of Ag/Z exhaustion, showed the values: 99.1, 99.6 and 99.8%. Antimicrobial activity against *C. albicans* was found to be insufficient when Ag/Z was tested, where for 24S, 06D and 24D samples cell inactivation was: 19.1, 20.9 and 24.5%, respectively. This is affected by the presence of Ag^+-ions which are

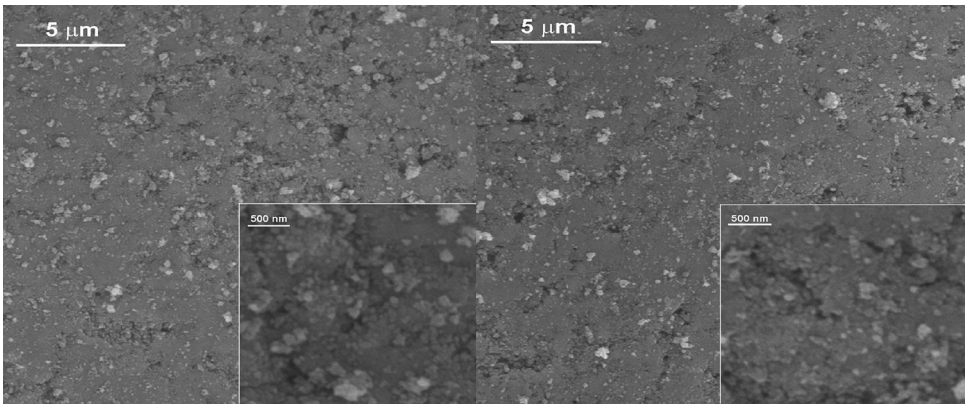

Fig. 11. FE-SEM image of T (on the left) and Ag/T (on the right) with 10,000 and 70,000 times enlargement (incorporated picture).

Table 4
Antimicrobial activity of Ag^+-ions on the solid phase (Ag/GAC, Ag/Z and Ag/T activated sorbents in different exhaustion stages), after 15 min of exposure period to microbial solution.

Sample	*E. coli*						*S. aureus*						*C. albicans*					
	CFU/mL			*R* (%)			CFU/mL			*R* (%)			CFU/mL			*R* (%)		
	24S	06D	24D	24S	06D	24D	24S	06D	24D	24S	06D	24D	24S	06D	24D	24S	06D	24D
Control GAC	3.98×10^5	3.98×10^5	3.98×10^5				6.00×10^5	6.00×10^5	6.00×10^5				2.20×10^5	2.20×10^5	2.20×10^5			
Ag/GAC	2.10×10^5	2.00×10^5	1.92×10^5	47.2 ± 0.3	49.7 ± 0.4	51.8 ± 0.3	3.30×10^5	3.10×10^5	3.00×10^5	45.0 ± 0.4	48.3 ± 0.3	50.0 ± 0.5	1.45×10^5	1.40×10^5	1.25×10^5	34.1 ± 0.2	36.4 ± 0.1	43.2 ± 0.3
Control Z	3.83×10^5	3.83×10^5	3.83×10^5				5.40×10^5	5.40×10^5	5.40×10^5				2.78×10^5	2.78×10^5	2.78×10^5			
Ag/Z	3.56×10^4	3.00×10^4	2.50×10^4	90.7 ± 0.2	92.2 ± 0.1	93.5 ± 0.1	5.10×10^3	2.20×10^3	1.10×10^3	99.1 ± 0.1	99.6 ± 0.2	99.8 ± 0.1	2.25×10^5	2.20×10^5	2.10×10^5	19.1 ± 0.4	20.9 ± 0.3	24.5 ± 0.4
Control T	3.45×10^5	3.45×10^5	3.45×10^5				5.00×10^5	5.00×10^5	5.00×10^5				2.70×10^5	2.70×10^5	2.70×10^5			
Ag/T	7.45×10^4	5.90×10^4	4.10×10^4	78.4 ± 0.2	82.0 ± 0.3	86.8 ± 0.2	1.05×10^5	7.45×10^4	5.20×10^4	79.0 ± 0.3	85.1 ± 0.4	89.6 ± 0.4	1.80×10^5	1.60×10^5	1.40×10^5	33.3 ± 0.3	40.7 ± 0.2	48.1 ± 0.2

incorporated and dispersed into the material. It was not only the concentration of the activating agent, since zeolite had the lowest sorption capacity for Ag^+-ions, comparing with GAC and T sorbents, as presented in Table 2, but also the accessibility and distribution of Ag^+-ions resulted in the efficient antimicrobial activity [5].

When testing Ag/T, activated sorbent the results were intermediate inhibition. The disinfection was 10% lower comparing to Ag/Z, despite the higher sorption capacity of Ag/T for Ag^+-ions, as shown in Table 2. The inhibition rate of Ag/T against *E. coli*, tested for 24S, 06D and 24D samples, increased in following order: 78.4, 82.0 and 86.8%, respectively. *S. aureus* cell inactivation provided by Ag/T, with respect to the order of tested samples (24S, 06D and 24D), was: 79.0, 85.1 and 89.6%., Comparing all three activated sorbent, removal of *C. albicans*, was the most efficient by Ag/T. The rate of antimicrobial activity increased for less loaded Ag/T samples. For 24S, 06D and 24D against *C. albicans* the inhibition rate was: 33.3, 40.7 and 48.1%, respectively. Structural analysis of Ag/T showed that silver is also doped as Ag^+-ion (in the chemical form of AgO), but probably the heterogeneous distribution of Ag^+-ions on the surface, as well as reduction of AgO on the surface [54], led to less efficient antimicrobial activity, compared to Ag/Z. The analysis of the inhibition rate is specially interesting from desorption aspect. Although Ag/T sorbent has 10 times more pronounced desorption rate than Ag/Z, antimicrobial activity of Ag/T did not extend 80%. This leads to the conclusion that inhibition is mostly the consequence of the contact between microbial and Ag^+-ions from activated surface sites and not Ag^+-ions detached from the surface.

When testing, Ag/GAC, this sorbent showed the lowest cell reduction against *E. coli*, *S aureus* and *C. albicans* (Table 4). Inhibition rate against *E. coli*, tested for 24S, 06D and 24D activated Ag/GAC samples was 47.2, 49.7 and 51.8%, respectively. Respecting the order of selected samples (24S, 06D and 24D), *S. aureus* cell reduction was similar as *E. coli* inhibition, with values: 45.0, 48.3, and 50.0%, while for *C. albicans* cell removal was less efficient, with values: 34.1, 36.4, and 43.2%. These results were expected due to the fact that silver ions from the activation medium were reduced when loaded on the GAC surface and Ag/GAC activate sites are filled by metallic silver. Elemental silver is known to be an ineffective inhibitor [43], but silver bactericidal effect depends on its bioavailability [40]. This fact implies that microbial cell reduction of Ag/GAC is consequence of Ag^+-ions release in the solution from Ag/GAC surface, during 15 min of exposure period. This will be further examined in the antimicrobial tests of the Ag^+-ions released from the activated surface. Furthermore, GAC and Z sorbent had the same desorption rate, which indicates their similar antimicrobial activity. On the other hand, Ag/Z sorbent proved to have double inhibition effects due to surface properties, as stated previously.

When antimicrobial data of the Ag^+-activated sorbents shown in Table 4, are analyzed, the microbial cell reduction for Ag/GAC activated sorbent is in ascending order from *C. albicans*, over *S. aureus* to *E. coli*, while for Ag/Z and Ag/T there is slight advantage for *S. aureus* cell reduction comparing to *E. coli*. For all three activated sorbents, *C. albicans* proved to be the most resistible microbe by silver inhibition. Different microbial species have different protective mechanism when exposed to chemical agent, e.g. different states of silver [30]. Among tested organisms, *E. coli* and *S. aureus* have shown high sensitivity upon exposure to silver (especially to Ag^+-ion, which is present on activated sites on Ag/Z and Ag/T sorbents). *C. albicans* cells can produce the antioxidative enzyme, catalase, which can protect the cell from degradation [55].

Another observation is related to the exhaustion period of the tested samples. It was noticed that more exhausted sorbents (the samples labeled as 06D and 24D) manifested slightly higher

antimicrobial activity, compared to the fresh activated ones (24S). This is probably related to the availability of the Ag^+-activated surface sites. The high Ag^+-ion loadings resulted in a reduction of the antimicrobial activity as described elsewhere [16,21]. The sorbent after 6 and 24 h of desorption period was more effective in antimicrobial activity than the maximum loaded one. There are two possible explanations, which are in agreement with studies of other authors: (i) this is due to the reduction of silver ions to elemental forms (from Ag^+ to Ag^0) [21] and (ii) the release of Ag^+-ions leads to increase in porosity of the material [18]. The higher Ag^+/Ag^0 ratio in activated material expressed better antimicrobial activity [41]. With the release of Ag^+ ions from the surface (after 6 and 24 h of exhausting period), there is much more free space on the surface that enables bacteria to 'grab on the surface', which improves the overall antimicrobial effect. Similar conclusions have been already reported [21].

3.4.2. Antimicrobial activity of Ag^+-ions in aqueous phase

As previously shown in desorption kinetic studies, tested Ag/GAC, Ag/Z and Ag/T sorbents have different affinities for releasing Ag^+-ions. Low desorption is characteristic for zeolite, intermediate rate for activated carbon and high desorption rate for titanium-dioxide sorbent. The selection of the sorbents with different desorption rates is made on purpose in order to follow the influence of free Ag^+-ions in aqueous solution. The antimicrobial efficacy of Ag^+-ions released in aqueous phase during desorption experiment could determine the contribution of desorbed ions to the overall antimicrobial activity. These conclusions could clarify the pathway of the antimicrobial activity of the activated sorbents.

This study was subjected to the controlled antimicrobial conditions, using free Ag^+-ions released from the Ag/GAC, Ag/Z and Ag/T sorbents. Sorbents were tested in different stages of their exhaustion, previously described in antimicrobial tests of the Ag^+-activated sorbents. Samples are labeled in the same manner: 24S-a (sorbent after 24 h of activation process), 06D-a (sorbent after 6 h of desorption process) and 24D-a (sorbent after 24 h of desorption process). Label 'a' stands for the concentration of Ag^+-ions in aqueous phase. Desorption period for all samples was limited to 15 min. This interval is equal to duration of the incubation period in antimicrobial tests of Ag^+-solid phase. The results of antimicrobial activity of released Ag^+-ions are presented in Table 4.

Ag/Z sorbent showed low desorption rate for Ag^+-ions after 15 min of desorption period. Solid samples in different exhaustion stages (24S, 06D, 24D) desorbed low quantities of Ag^+-ions in aqueous phase (24S-a, 06D-a, 24D-a). The values obtained are expressed in mg/L: 0.080, 0.030 and 0.020, respectively. The concentrations of Ag^+-ions desorbed from Ag/GAC sorbent were 10 times higher than those of Ag/Z, collected in the same interval. The values for Ag/GAC samples, with respect to their order (24S-a, 06D-a, 24D-a) are: 0.500, 0.200 and 0.035 mg/L, respectively. Ag/T sorbent showed extremely good release of Ag^+-ions, with values of 5.00, 0.400 and 0.170 mg/L after 15 min of desorption period, for collected samples: 24S-a, 06D-a and 24D-a, respectively.

Results indicate that, similar to the order of the antimicrobial activity of Ag^+-ions from the activated sorbents, the most sensitive to the presence of Ag^+-ions in aqueous phase were *S. aureus*, and *E. coli* [9], while *C. albicans* was the most resistible one. The cell reduction of Ag^+-ions from aqueous phase (see Table 5) was performed in separate antimicrobial experiment, related only to the concentration of free Ag^+-ions in the microbial solution. As expected, cell removal decreased as the concentration of Ag^+-ions decreased, for the analyzed aqueous samples: 24S-a, 06D-a and 24D-a. The best cell removal for all three microbes was obtained for Ag/T aqueous samples, due to the highest desorption rate. In general, antimicrobial activity of Ag^+-ions desorbed from the Ag/GAC, Ag/Z and Ag/T activated sorbents is low because of the

Table 5
Antimicrobial activity of released Ag^+-ions in aqueous phase (from the activated sorbents in different exhaustion stages), after 15 min of exposure period to microbial solution.

Sample	*E. coli*					*S. aureus*					*C. albicans*				
	CFU/ml			R (%)		CFU/ml			R (%)		CFU/ml			R (%)	
	24Sa	06Da	24Da	24Sa	06Da	24Da	24Sa	06Da	24Da	24Sa	06Da	24Da	24Sa	06Da	24Da
Control saline solution	2.12×10^6	2.12×10^6	2.12×06				1.35×10^6	1.35×10^6	1.35×10^6				1.43×10^6	1.43×10^6	1.43×10^6
Ag/GAC	1.65×10^6	1.78×10^6	1.95×10^6	22.2 ± 0.3	16.0 ± 0.2	8.0 ± 0.1	1.07×10^6	1.10×10^6	1.21×10^6	20.7 ± 0.2	18.5 ± 0.2	10.4 ± 0.1	1.22×10^6	1.37×10^6	1.41×10^6	14.7 ± 0.2	4.2 ± 0.2	1.4 ± 0.1
Ag/Z	1.98×10^6	2.00×10^6	2.05×10^6	6.6 ± 0.1	5.7 ± 0.1	3.3 ± 0.1	1.25×10^6	1.30×10^6	1.32×10^6	7.4 ± 0.1	3.7 ± 0.1	2.2 ± 0.1	1.38×10^6	1.40×10^6	1.39×10^5	3.5 ± 0.2	2.1 ± 0.2	2.8 ± 0.2
Ag/T	1.35×10^6	1.65×10^6	1.75×10^6	36.3 ± 0.3	22.2 ± 0.2	17.5 ± 0.2	8.00×10^5	1.02×10^6	1.18×10^6	40.7 ± 0.4	24.4 ± 0.3	12.6 ± 0.2	1.05×10^6	1.20×10^6	1.35×10^5	26.6 ± 0.3	16.2 ± 0.2	5.6 ± 0.1

short exposure period (15 min) of activating agent to the microbial solution (see Table 5).

3.4.3. Overall antimicrobial activity

Overall antimicrobial activity of Ag/GAC, Ag/Z and Ag/T activated sorbents could be explained through divided antimicrobial tests of Ag^+-ions from the solid phase and Ag^+-ions from the aqueous phase. The most important aspect of this investigation is related to the different desorption rates of the selected and tested materials, which enabled to examine and follow the changes in Ag^+-aqueous and Ag^+-solid microbe interactions. Regarding Ag/Z sorbent, where low desorption rate is observed and due to neglecting antimicrobial activity of released Ag^+-ions (as shown in Table 5), the conclusion is that an overall cell reduction is a consequence of Ag^+-activated sites on the surface. Despite this, Ag/T with high desorption rate has significant contribution of Ag^+-ions that are desorbed from the activated surface to an overall inhibition. Comparing the inhibition rate of 24S (Ag^+-activated T, Table 4) and 24S-a (Ag^+-ions desorbed from Ag/T, Table 5) samples, almost 50% of the total cell reduction is related to the presence of Ag^+-ions in aqueous phase. The high desorption of Ag^+-ions from the Ag/T activated surface after 15 min of desorption was significant to exhibit how this result. Similar observation can be made for Ag/GAC antimicrobial analysis, where Ag^+-ions were loaded as elemental silver (Ag^0) on the GAC surface, which additionally confirms the antimicrobial effect of released Ag^+-ions. But, it is important to point out that influence of Ag^+-ions from the aqueous phase is the most dominant for the fresh activated sorbents, with maximum Ag^+-loading (samples marked as 24S, in Table 4), where the change of the content of released Ag^+-ions with time is the greatest (24S-a, in Table 5). Samples after exhaustion period (samples marked as 06D and 24D, in Table 4) have slower desorption kinetics and the release of Ag^+-ions is, as expected, less expressed. For these samples, the contribution of Ag^+-ions in cell removal (Table 5) is less expressed and the most of the antimicrobial activity belongs to the effect of Ag^+-activated surface sites (Table 4).

Observing all interpreted results and discussions, enclosing the activating agent and its chemical state, structural properties of the activated sorbents, separate antimicrobial analysis of the Ag^+-ions in the aqueous and Ag^+-ions from the solid phase, there is a strong scientific belief that the overall antimicrobial effect is not only related to the presence and quantity of Ag^+-ions, but also is affected by the surface properties of the samples. The clarification of this phenomena and mechanisms of antibacterial activity on the sorbent surface will be a focus of further investigations in this field of the research.

4. Conclusions

This research is focused on antimicrobial activity of Ag^+-activated sorbents. Sorption and desorption capacities were important criteria for the selection of proper and suitable materials: zeolite, granular activated carbon, and titanium dioxide. The Ag^+-activated sorbents were examined in antimicrobial tests against *E. coli*, *S. aureus* and *C. albicans*. The greatest inhibition rate, after 15 min of exposure period, was obtained for Ag-zeolite vs. *S. aureus* and *E. coli*, 99.8 and 93.5%, respectively. For all activated sorbents, the lowest removal efficacy is obtained against *C. albicans*. Structural analysis of the activated sorbents gave insights into the chemical state of the silver activating agent, which reflects greatly their antimicrobial efficacy. The XRD, XPS and FE-SEM analysis confirmed that silver in Ag-granular activated carbon was in elemental form (Ag^0), in Ag-titanium-dioxide was in ionic state (Ag^+), while in Ag-zeolite was in elemental (Ag^0) and ionic state (Ag^+). This was confirmed in antimicrobial tests, where Ag-granular activated carbon had the lowest removal rate, for all three tested microbial.

The pathway of the antimicrobial activity was of specific interest in this study. The antimicrobial activity of the activated sorbents have been observed through two different aspects: the inhibition rate of the Ag^+-ions loaded on the surface activated sites and the contribution of the free Ag^+-ions released from the activate surface into aquatic environment. Separately, antimicrobial tests were performed to demystify the contribution of the solid phase, activated surface, in total antimicrobial activity. The results indicated that antimicrobial performance of activated sorbents depends not only on the concentration of the activating agent, but also on the surface characteristics of the material, which directly determines the distribution and the accessibility of the activating agent. This research is an attempt to alleviate the discussion on antimicrobial effect of silver activated materials. Moreover, this paper gives a strong theoretical and empirical baseline for further development and application of different active sorption and filtration media.

Acknowledgements

This work was financial supported by grants by the Ministry of Education and Science of the Republic of Serbia (III 43009). The authors would like to acknowledge the financial support provided by COST-European Cooperation in Science and Technology, to the Cost Action 1403: New and Emerging challenges and opportunities in wastewater reuse (NEREUS).

References

[1] T.K. Sen, D. Gomez, Adsorption of zink (Zn^{2+}) from aqueous solution on natural bentonite, Desalination 267 (2011) 286–294.
[2] A. Djukić, U. Jovanović, T. Tuvić, V. Andrić, J. Grbović Novaković, N. Ivanović, L.J. Matović, The potential of ball-milled Serbian natural clay for removal of heavy metal contaminants from wastewaters: Simultaneous sorption of Ni, Cr, Cd and Pb ions, Ceram. Int. 39 (2013) 7173–7178.
[3] M.E. Ramos, F.J. Huertas, Adsorption of glycine on montmorillonite in aqueous solutions, Appl. Clay Sci. 80–81 (2013) 10–17.
[4] J. Hrenovic, J. Milenkovic, T. Ivankovic, N. Rajic, Antibacterial activity of heavy metal-loaded natural zeolite, J. Hazard. Mater. 201–202 (2012) 260–264.
[5] D.J. Stojakovic, J. Hrenovic, M. Mazaj, N. Rajic, On the zink sorption by the Serbian natural clinoptilolite and the disinfecting ability and phosphate affinity of the exhausted sorbent, J. Hazard. Mater. 185 (2011) 408–415.
[6] T.Q. Tuan, N.V. Son, H.T.K. Dung, N.H. Luong, B.T. Thuyb, N.T.V. Anhb, N.D. Hoac, N.H. Haia, Preparation and properties of silver nanoparticles loaded in activated carbon for biological and environmental applications, J. Hazard. Mater. 192 (2011) 1321–1329.
[7] P.C. Mishra, R.K. Patel, Removal of lead and zink ions from water by low cost sorbents, J. Hazard. Mater. 168 (2009) 319–325.
[8] E. Katsou, S. Malamis, K. Haralambous, Examination of zink uptake in a combined system using sludge, minerals and ultrafiltration membranes, J. Hazard. Mater. 182 (2010) 27–38.
[9] J.L. Clement, P.S. Jarrett, Antibacterial silver, Met.-Based Drugs 1 (1994) 467–482.
[10] R. Zhu, L. Zhu, J. Zhu, L. Xu, Structure of surfactant–clay complexes and their sorptive characteristics toward HOCs, Sep. Purif. Technol. 63 (2008) 156–162.
[11] S. Komarneni, A.R. Aref, S. Hong, Y.D. Noh, F.S. Cannon, Y. Wang, Organoclays of high-charge synthetic clays and alumina pillared natural clays: perchlorate uptake, Appl. Clay Sci. 80–81 (2013) 340–345.
[12] Y.I. Li, A. Deletic, D.T. McCarthy, Removal of *E. coli* from urban storm water using antimicrobial-modified filter media, J. Hazard. Mater. 271 (2014) 73–81.
[13] Unites States Environmental Protection Agency, EPA, Edition of the Drinking Water Standards and Health Advisors, EPA 820-R-11-002, Office of Water U.S. Environmental Protection Agency, Washington, DC, 2011.
[14] World Health Organization (WHO), Guidelines for Drinking Water Quality, vol. 2, WHO, Geneva, 1996.
[15] Directive 2006/7/EC of the European Parliament and of the Council of 15 February 2006 concerning the management of bathing water quality and repealing Directive 76/160/EEC, Off. J. Eur. Union, L64/37.
[16] M. Rivera-Garza, M.T. Olguin, I. Garcia-Sosa, D. Alcantara, G. Rodriguez-Fuentes, Silver supported on natural Mexican zeolite as an antimicrobial material, Microporous Mesoporous Mater. 39 (2000) 431–444.
[17] Y. Matsumura, K. Yoshikata, S. Kunisaki, T. Tsuchido, Mode of bactericidal action of silver zeolite and its comparison with that of the silver nitrate, Appl. Environ. Microbiol. 69 (2003) 4278–4281.

[18] S.M. Magana, P. Quintana, D.H. Aguilar, J.A. Toledo, C. Angeles-Chavez, M.A. Cortes, L. Leon, Y. Freile-Pelegrin, T. Lopez, R.M. Torres Sanchez, Antibacterial activity of montmorillonites doped with silver, J. Mol. Catal. A: Chem. 281 (2008) 192–199.
[19] Y. Innoue, M. Kogure, K. Matsumoto, H. Hamashima, M. Tsukada, K. Endo, T. Tanaka, Light irradiation is a factor in the bactericidal activity of silver-loaded zeolite, Chem. Pharm. Bull. 56 (2008) 692–694.
[20] Z. Milan, C. de las Pozas, M. Crus, R. Borja, E. Sanchez, K. Ilangovan, Y. Espinosa, B. Luna, The removal of bacteria by modified natural zeolites, J. Environ. Sci. Health Part A: Tox. Hazard. Subst. Environ. Eng. 36 (2001) 1073–1087.
[21] A. Top, S. Ulku, Silver, zink, and copper exchange in a Na-clinoptilolite and resulting effect on antimicrobial activity, Appl. Clay Sci. 27 (2004) 13–19.
[22] B. Kwakye-Awuah, C. Williams, M.A. Kenward, I. Radecka, Antimicrobial action and efficiency of silver-loaded zeolite X, J. Appl. Microbiol. 104 (2008) 1516–1524.
[23] K. Malachova, P. Praus, Z. Rybkova, O. Kozak, Antibacterial and antifungal activities of silver, copper and zinc montmorillonites, Appl. Clay Sci. 53 (2011) 642–645.
[24] A. Esteban-Cubillo, C. Pecharroman, E. Aguilar, J. Santaren, J.S. Moya, Antibacterial activity of copper monodispersed nanoparticles onto sepiolite, J. Mater. Sci. 41 (2006) 5208–5212.
[25] L. Korosi, S. Papp, J. Menesi, E. Illes, V. Zollmer, A. Richardt, I. Dekary, Photocatalytic activity of silver-modified titanium-dioxide at solid–liquid and solid–gas interferences, Colloids Surf. A 319 (2008) 136–142.
[26] E.A. Al-Arfaj, Structure and photocatalysis activity of silver doped titanium oxide nanotubes array for degradation of pollutants, Superlattices Microstruct. 62 (2013) 285–291.
[27] A. Garcia, L. Delgado, J.A. Tora, E. Casals, E. Gonzalez, V. Puntes, X. Font, J. Carrera, A. Sanchez, Effect of cerium dioxide, titanium dioxide, silver, and gold nanparticles on the activity of microbial intended in wastewater treatment, J. Hazard. Mater. 199–200 (2012) 64–72.
[28] M.V. Liga, E.L. Bryant, V.L. Colvin, Q. Li, Virus inactivation by silver doped titanium dioxide nanparticles for drinking water treatment, Water Res. 45 (2011) 535–544.
[29] B. Lin, Y. Luo, Z. Teng, B. Zhang, B. Zhou, Q. Wang, Development of silver/titanium dioxide/chitosan adipate nanocomposite as an antibacterial coating for fruit storage, LWT – Food Sci. Technol. 63 (2015) 1206–1213.
[30] I.D. Vukoje, T.D. Tomasevic-Ilic, A.R. Zarubica, S. Dimitrijevic, M.D. Budimir, M.R. Vranjes, Z.V. Saponja, J.M. Nedeljkovic, Silver film on nanocrystalline TiO_2 support: photocatalytic and antimicrobial ability, Mater. Res. Bull. 60 (2014) 824–829.
[31] M. Ulmanu, I. Anger, E. Gament, G. Olanescu, C. Predescu, M. Sohaciu, Effect of a Romanian zeolite on heavy metals transfer from polluted soil to corn, mustard and oat, U.P.B. Sci. Bull. Ser. B 68 (3) (2006) 67–78.
[32] B.M. Jovanović, V.I. Vukašinović-Pešić, Đ.N. Veljović, Lj.V. Rajaković, Arsenic removal from water using low-cost adsorbents – a comparative study, J. Serb. Chem. Soc. 76 (10) (2011) 1437–1452.
[33] V. Tomašić, I. Brnardić, H. Jenei, V. Kosar, S. Zrnačević, Combustion of active carbon as a model carbon material: comparison of non-catalytic and catalytic oxidation, Chem. Biochem. Eng. Q. 25 (3) (2011) 283–287.
[34] D.D. Milenković, Lj.V. Rajaković, S. Stoiljković, The sorption of cyanides from the water onto activated carbon, Facta Univ. Ser.: Work. Living Environ. Prot. 2 (4) (2004) 251–258.
[35] ADSORBSIA AS600, Titanium Based Adsorbent Material Safety Data Sheet, The Dow Chemical Company http://www.dowwaterandprocess.com/en/Products/A/ADSORBSIA_AS600 (last access 02.08.15).
[36] A. Sari, M. Tuzen, Adsorption of silver from aqueous solution to onto raw vermiculite and manganese oxide-modified vermiculite, Microporous Mesoporous Mater. 170 (2013) 155–163.
[37] E.S. Gould, Inorganic Reactions and Structure, rev. ed., Stanford Research Institute, Holt, Rinehart and Winston – New York, 1962.
[38] M.B. Đolić, V.N. Rajaković-Ognjanović, J.P. Marković, L.J. Janković-Mandić, M.N. Mitrić, A.E. Onjia, Lj.V. Rajaković, The effect of different extractants on lead desorption from natural minerals, Appl. Surf. Sci. 324 (2015) 221–231.
[39] K. Malachova, P. Praus, Z. Pavlickova, M. Turicova, Activity of antibacterial compounds immobilised on montmorillonite, Appl. Clay Sci. 43 (2009) 364–368.
[40] P. Lalueza, M. Monzon, M. Arruebo, J. Santamaria, Bactericidal effects of different silver-containing materials, Mater. Res. Bull. 46 (2011) 2070–2076.
[41] L. Ferreira, A.M. Fonseca, G. Botelho, C. Almeida-Aguiar, I.C. Neves, Antimicrobial activity of faujasite doped with silver, Microporous Mesoporous Mater. 160 (2012) 126–132.
[42] D.W. Brett, A discussion of silver as an antimicrobial agent: alleviating the confusion, Ostomy/Wound Man. 52 (2006) 34–41.
[43] Y. Inoue, H. Hamashima, Electrochemical analysis of the redox state of silver contained in antibacterial material, J. Biomater. Nanobiotechnol. 3 (2012) 136–139.
[44] H. Ortiz-Ibarra, N. Casillas, V. Soto, M. Barcena-Soto, R. Torres-Vitela, W. de la Cruz, S. Gómez-Salazar, Surface characterization of electrodeposited silver on activated carbon for bactericidal purposes, J. Colloid Interface Sci. 314 (2007) 562–571.
[45] Y. Zhao, Z. Wang, X. Zhao, W. Li, S. Liu, Antibacterial action of silver-doped activated carbon prepared by vacuum impregnation, Appl. Surf. Sci. 266 (2013) 67–72.
[46] L. Jiang, F. Wang, F. Han, W. Prinyawiwatkul, H.K. No, B. Ge, Evaluation of diffusion and dilution methods to determine the antimicrobial activity of water-soluble chitosan derivatives, J. Appl. Microbiol. 114 (3) (2013) 956–963.
[47] Y.F. Jia, C.J. Steele, I.P. Hayward, K.M. Thomas, Mechanism of adsorption of gold and silver species on activated carbons, Carbon 36 (1998) 1299–1308.
[48] H.-L. Feng, X.-Y. Gao, Z.-Y. Zhang, J.-M. Ma, Study on the crystalline structure and the thermal stability of silver-oxide films deposited by using direct-current reactive magnetron sputtering methods, J. Korean Phys. Soc. 54 (4) (2010) 1176–1179.
[49] N.N. Greenwood, A. Earnshaw, Chemistry of the Elements, 2rd ed., Butterworth-Heinemann, 1997, ISBN 0080379419.
[50] R.J. Bird, P. Swift, Energy calibration in electron spectroscopy and the re-determination of some reference electron binding energies, J. Electron Spectrosc. Relat. Phenom. 21 (1980) 227–240.
[51] X. Tang, J. Chen, Y. Li, Y. Li, Y. Xu, W. Shen, Complete oxidation of formaldehyde over Ag/MnO_x–CeO_2 catalysts, Chem. Eng. J. 118 (2006) 119–125.
[52] J.A. Jiménez, H. Liu, E. Fachini, X-ray photoelectron spectroscopy of silver nanoparticles in phosphate glass, Mater. Lett. 64 (2010) 2046–2048.
[53] L. Korosi, Sz. Papp, I. Bertoti, I. Dekany, Surface and bulk composition, structure, and photocatalytic activity of phosphate-modified TiO_2, Chem. Mater. 19 (2007) 4811–4819.
[54] X. Zou, J. Shi, H. Zhang, Coexistence of silver and titanium dioxide nanoparticles: enhancing or reducing environmental risk? Aquat. Toxicol. 154 (2014) 168–175.
[55] C.E.B. Linares, D. Briebeler, D. Cargnelutti, S.H. Alves, V.M. Morsch, M.R.C. Schetinger, Catalase activity in *Candida albicans* exposed to antineoplastic drugs, J. Med. Microbiol. 55 (2006) 259–262.